VALIDATION OF AN A PRIORI AERODYNAMIC MODEL BASED ON CFD RESULTS

W.G.M. Vos, H. Bijl, J.M. Cnossen, L.L.M. Veldhuis, J. Oliveira
Delft University of Technology,
Delft, The Netherlands

1. Introduction

At the Delft University of Technology a joint project between between the Control and Simulation (C&S) and the Aerodynamics (AD) groups was started in the area of ight simulation. The goal is to develop a new method to generate Flight Simulation Models (FSM) where an a priori aerodynamic model (AAM) based on Computational Fluid Dynamics (CFD) computations is updated by means of an Aerodynamic Residual Model (ARM). This ARM is obtained by combining the AAM with the results gained from ight tests. The AAM will provide a structure for the function that returns aerodynamic forces and moments, i.e. the AAM will bring forth the most important input dependencies that best parametrises the function.

To get to an FSM the aerodynamic characteristics of the full scale aircraft have to be known. While these characteristics are generally computed through ight tests identi cation (FTI) in this project CFD is used to provide the data. A FSM model of the Cessna Citation II is developed to test if the FSM can be generated in a faster and cheaper way using the proposed new method instead of the classic methods based completely on FTI [5].

At this moment Euler computations are done for steady, symmetric ight conditions to gain con dence in the CFD results. In this paper the accuracy of aerodynamic coef cients based on preliminary CFD calculations using the Euler equations is related with the accuracy FTI results. Only when these accuracies agree well and have the same order of magnitude using CFD in the construction of an aerodynamic model is meaningful. When in future work the CFD data will actually be used for the generation of an AAM also Navier-Stokes computations of the Cessna Citation II will be considered.

In this paper rst the geometrical model is discussed. This part covers the three dimensional CAD model as well as the grid generation. Then the size of the computational domain and its relation to the accuracy of the results is discussed. The o w solver based on the Euler equations and the boundary conditions are discussed next. Since we use a simpli ed engine model this model needs to be explained. Finally the Euler results are presented and validated with FTI results.

2. CAD Modelling and Grid Generation

A three dimensional CAD model of the Cessna Citation II has been created with a commercial CAD system (Rhinoceros NURBS 3D modeling) following the same methods as Fujita et al. [2]. For this paper only half a model, as shown in Fig. 1, is used since the computations are done for steady symmetric ight. Separating the Citation II model into different parts (fuselage, wing, horizontal stabiliser, pylon, nacelle) makes it easy to modify one part without a need to change the complete model. In this way different aircraft con gurations can be generated in a short period of time. An all hexahedral unstructured grid is used to discretise the o w domain. To obtain short setup time mesh generation is performed automatically with the grid generator (Hexpress^{TM}) of NUMECA International. Since small surfaces might lead to problems in an automatic grid generation (the trailing edge of the Citation II has a nite thickness of less than one percent of the aerodynamic chord of the wing) the trailing edge was sharpened.

3. The Computational Domain

The size of the computational domain around the three dimensional model of the Cessna Citation II, is determined by the desired accuracy of the CFD results for the construction of an AAM. Since this paper only focuses on steady symmetric ight conditions one border of the computational domain is the mirror plane of the aircraft (XZ-plane, see gure Fig. 1). The three sizes of the domain that need to be determined are the width (in Y-direction), the length (in X-direction) and the height (in Z-direction).

The width of the domain is determined by the in uence of the side border (gray plane in Fig. 1) of the computational domain on the angle of attack at the wing. A way to estimate this in uence is to replace the aircraft by a horseshoe vortex, as described in many standard works, with a bound vorticity strength of:

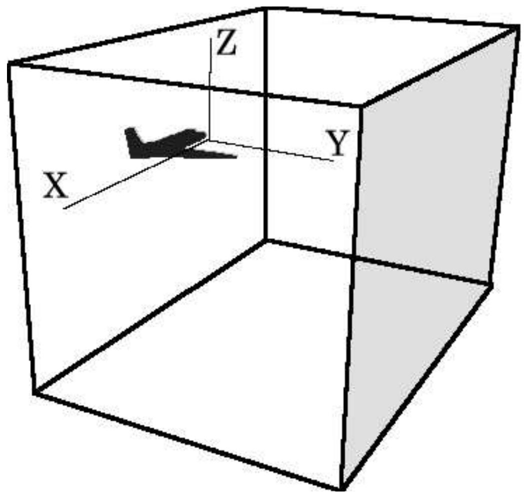

Fig. 1. Computational domain

$$\Gamma = \frac{L}{\rho V b}. \tag{1}$$

Here L is the lift, ρ is the density, V is the velocity and b is the span. This vortex is mirrored and opposed with respect to the side of the box. This mirrored horseshoe vortex changes the vertical velocity, hence the angle of attack at the wing. The change in vertical velocity is equal to:

$$\Delta V = \frac{\Gamma}{4\pi h} \tag{2}$$

where h is the shortest distance from the mirrored horseshoe vortex to the wing. We rewrite equations (1) and (2) and introduce the con - dence interval for the angle of attack ($\alpha \pm \Delta\alpha$) coming from ight tests. The following equation gives the width of the computational domain that is needed to provide an angle of attack in the CFD results within the same con dence interval:

$$\text{width} = \frac{\Gamma}{8\pi \left(V_{x_\infty} \tan\beta - V_{z_\infty}\right)} + \frac{b}{2}. \tag{3}$$

Here V_{x_∞} and V_{z_∞} are the velocities in X- and Z-direction respectively, and $\beta = (\alpha - \Delta\alpha)$ is the con dence interval. Values for lift, velocity

and angle of attack change for every point in the steady symmetric flight envelope. So the width of the computational domain is the maximum value obtained with equation (3) for all points of the flight envelope.
To determine the length and height of the computational domain a two dimensional CFD analysis was done on the main airfoil of the Cessna Citation II, i.e. the root wing airfoil (NACA23014). At first the computational domain is taken 'sufficiently large'. This means that the influence of the borders on c_l and c_d[1] is negligible. To check if this is indeed true, the CFD values for c_l and c_d are compared with the results of a potential code (updated with a boundary layer model) for two dimensional airfoils [1]. If the results are the same the computational domain is 'sufficiently large'. Now we reduce the size of the computational domain and compare the results for c_l and c_d with the results obtained with the 'sufficiently large' computational domain. An error in c_l and c_d due to the influence of the borders is noticeable. Fig. 2 shows this influence for c_l. The smallest bounding box with errors in c_l and c_d within the confidence interval for C_L and C_D from flight tests provides results accurate enough with the smallest allowable domain which leads to a minimal computational time. To make sure that the computational domain is large enough for all points of the flight envelope, the two dimensional CFD analysis is done for these points in the flight envelope that give the largest errors in C_L and C_D (high angle of attack, high velocity, high pressure, high density). Since in a three dimensional situation pressure is relieved through the third dimension this two dimensional analysis can be considered to be too strict.
Using equation (3) to compute the width of the domain for an accuracy in angle of attack of $0.01°$ and taking an accuracy for c_l of less than 0.005 in the two dimensional analysis (see Fig. 2 the dimensions of the computational domain are determined.

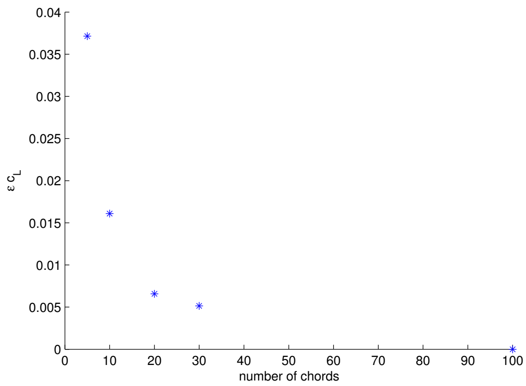

Fig. 2. Error in c_l in two dimensions as function of the size of the computational domain

The computational domain in this work has a length of 60 chords, a height of 60 chords and a width of 40 chords. The automatic grid generation led to 502583 cells in the domain.

4. The Flow Solver

The computations are done with the flow solver *Hexstream*^{TM} of NUMECA International. Steady Euler equations are solved with a second order central dicretisation scheme with Jameson-type artificial dissipation [4]. Local time stepping (4-stage explicit Runge-Kutta scheme) is used together with a multigrid strategy (3 grids, coarse grid initialisation) to march the governing equations in time towards the steady state solution [6].

5. Boundary Conditions

The fluid is modeled as perfect gas and on the boundaries of the computational domain undisturbed flow conditions are imposed. Furthermore on the engine inlet the pressure is defined, on the engine outlet velocity, temperature and mass flow are defined. In the next section the boundary conditions for the engine in- and outlet are discussed

[1] c_l and c_d are two dimensional coefficients while C_L and C_D are the corresponding three dimensional coefficients.

6. Simplified Engine Model

CFD techniques for turbomachinery make it possible to perform CFD computations throughout the engine of an aircraft. However, these computations are very time consuming especially when the interaction between the o w within the engine and around the aircraft is taken into account properly. Furthermore we do not expect a signi cant increase in accuracy using a complete engine model instead of a simpler model. The presence of working engines in the CFD model however, has a major in uence on the accuracy of the results.

Therefore a simpli ed engine model is developed. The turbofan engines are replaced by a black box with an inlet and an outlet. The inlet of the black box is chosen at the position of the fan, the outlet in the mixing plane of the hot and cold exhaust. To derive the boundary conditions at the inlet (p) and outlet ($\dot{m}$, T, V), needed for the CFD model, an engine model was developed along the lines of [3]. This simpler model introduces an error in the results but its detrimental effects is acceptable for the sake of the reduction of the computation time.

The inlet condition (p_{inlet}) is computed from the mass o w throughout the engine ($\dot{m}$) given by the Estimated Engine Performance Program (EEPP), developed by Pratt & Whitney, and the standard isentropic relations.

The outlet conditions (T_{outlet}, V_{outlet}) are computed assuming that we have straight out o w ($p_{\text{outlet}} = p_\infty$) from the engine. Assuming straight out o w means that all thrust has to be generated by the accelerated mass o w:

$$F_T = \dot{m}(V_{\text{outlet}} - V_\infty) \tag{4}$$

Using equation (4) V_{outlet} is computed.

The last boundary condition to be computed is T_{outlet}. Assuming that the energy o w of the (mixed) exhaust is the sum of the energy o ws in the cold and hot exhaust gives:

$$\dot{Q}_{\text{outlet}} = \dot{Q}_{\text{hot}} + \dot{Q}_{\text{cold}} \tag{5}$$

where $\dot{Q}$ equals:

$$\dot{Q} = \dot{m}(T_{\text{t}} - T_{\text{t}_\infty})c_{\text{p}} \tag{6}$$

Rewriting these equations gives an expression for $T_{\text{t}_{\text{outlet}}}$:

$$T_{\text{t}_{\text{outlet}}} = T_{\text{t}_\infty} + \frac{\dot{Q}_{\text{hot}} + \dot{Q}_{\text{cold}}}{\dot{m}_{\text{outlet}} c_{\text{p}}} \tag{7}$$

The standard isentropic relations now give the value for T_{outlet}.

7. Results

In this section we present results for a speci c part of the ight envelope where ight test data are currently available to enable a validation of the CFD results. Fig. 3 shows the ight envelope for the Cessna Citation II with the points in this ight envelope for which ight test results are available. The lines give the borders of the ight envelope and the dots mark the position of the ight test data points.

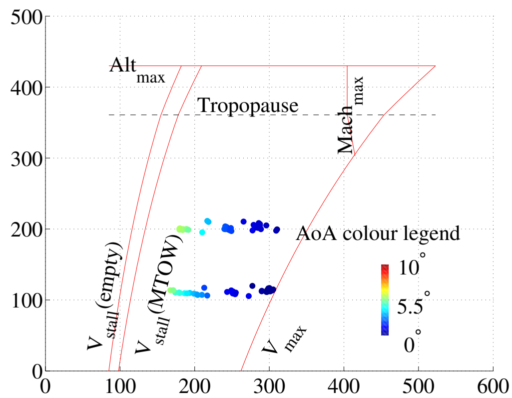

Fig. 3. Flight envelope of the Cessna Citation II (X-axis: velocity [kt], Y-axis: height [ight level])

Results are obtained for two types of engine models, i.e. " o w through" nacelles and engines on modeled as described in the previous section. All results are presented in the form of C_{L}-α and C_{D}-α curves.

Flow Through Nacelle

For the zero thrust case the engines were modeled as o w through nacelles. For all data points in Fig. 3, C_{L} and C_{D} are computed with the previously described CFD model. Fig. 4 shows these results in the form of C_{L}-α and C_{D}-α curves. The trendlines are extracted from the data points using a standard Least Squares Estimation. Since all the FTI data points have an angle of attack $\alpha < 7°$ we are far away from the stall area (α=10°) and the C_{L}-α curve is assumed to be linear. The C_{D}-α is expected to have a quadratic trend. This behaviour is clearly visible in Fig. 4. However a difference in lift curve slope between CFD and FTI is noticeable.

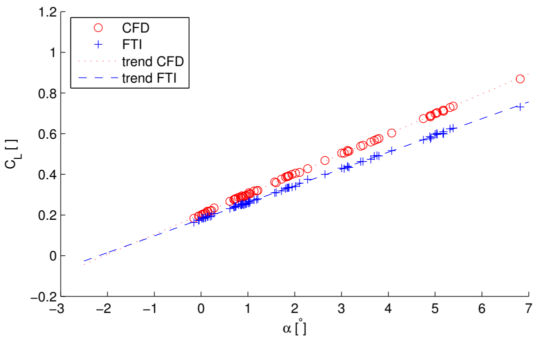

(a) C_{L}-α

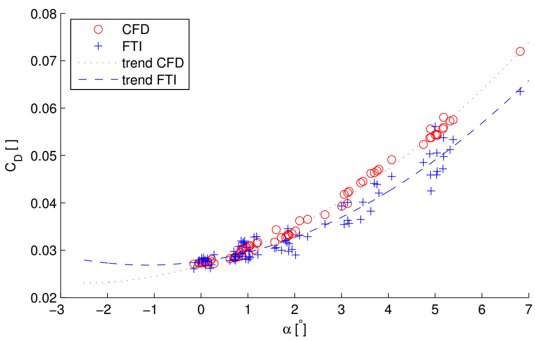

(b) C_{D}-α

Fig. 4. Comparison of the lift and drag curves (o w through nacelle)

This difference is due to the fact that the Euler equations do not incorporate viscous effects. Hence no effective decambering of the airfoil occurs due to the boundary layer. To show that this is indeed true the Euler CFD results were corrected for two dimensional viscous effects. Using a potential code (updated with a boundary layer model) for two dimensional airfoils [1] the relative error between the viscous and inviscid c_{l} is computed for the average wing airfoil of the Cessna Citation II. Adding this relative error (two dimensional) to the three dimensional CFD results for C_{L} shows indeed a clockwise rotation in the slope of the C_{L}-α as can be seen in Fig. 5. The correction is visualised for the trendlines (Least Squares Estimation). Also for C_{D} this approach leads to a shift of the C_{D}-α curve. This method is a very rough way to show that the difference in the slopes are indeed due to the fact that we use inviscid Euler equations instead of viscous Navier-Stokes equations.

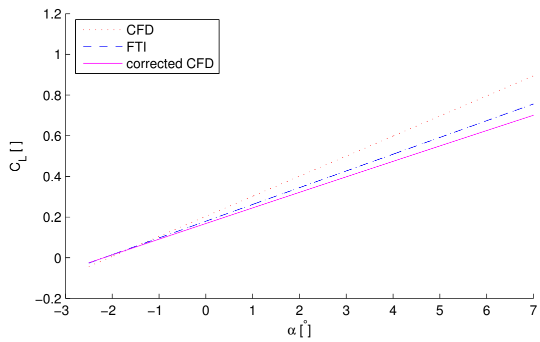

Fig. 5. Lift curve for corrected CFD data (o w through nacelle)

Engines On

The engine model described above is now applied. For the ight test data points in Fig. 3, C_L-α and C_D-α curves computed with this new CFD model are shown in Fig. 6. In the C_D-α curve a quadratic trend can be discovered, however, the computed C_D values seem to have a large deviation from this quadratic trend. This is because the engine model has an accuracy in Mach number of only 0.1. This causes large scatter in the thrust calculation, which is immediately translated into the (effective) drag results (C_D).

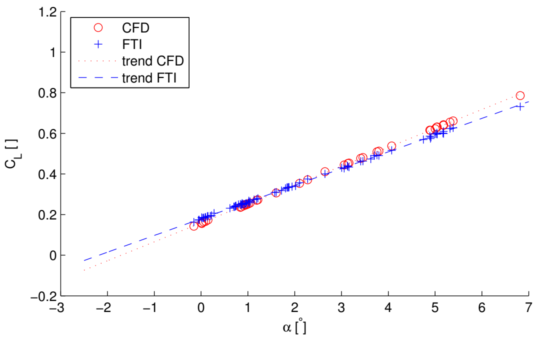

(a) C_L-α

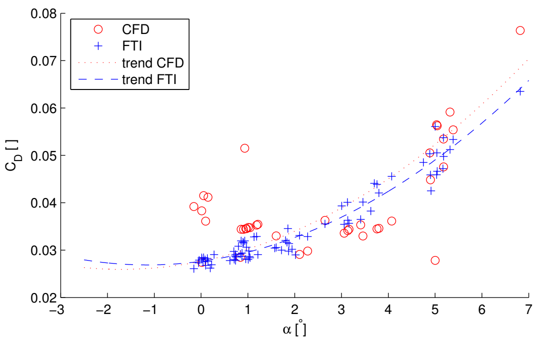

(b) C_D-α

Fig. 6. Lift and drag curves (engines on)

Using the same technique as described above for the o w through nacelle, the computed Euler CFD values for C_L and C_D can be corrected for two dimensional viscous effects. This causes again a change in the slope of the computed lift and drag curves in the direction of the measured (FTI) lift and drag curves.

Validation

For the validation of the Euler results (power off, engines on) the CFD data are compared with the FTI data. As can be seen from Fig. 4 and Fig. 6, Euler computations provide results that have similar trends as the FTI results. Adding an engine model increases the overall accuracy of the results but the C_D values show large deviations. Since the large deviations in C_D are expected to improve with an increase in accuracy of the Mach number for the engine model, special attention will be paid to the development of this model in the future.

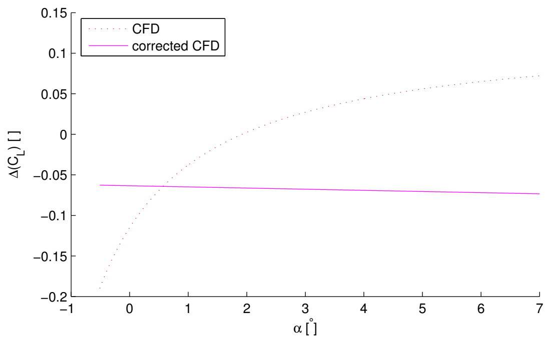

(a) C_L-α

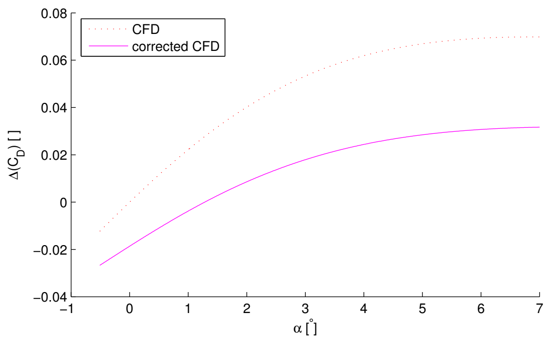

(b) C_D-α

Fig. 7. Relative difference between FTI and CFD results, engines on

Fig. 7 shows the relative difference between FTI and CFD results. This difference is de ned as:

$$\frac{S_\mathrm{FTI} - S_\mathrm{X}}{S_\mathrm{FTI}}. \tag{8}$$

Here S can be C_L or C_D and X is indicates which CFD results (corrected or not) are used. After a correction for two dimensional viscous effects the difference between CFD en FTI results (trendlines) becomes almost a factor two smaller. The Euler results are within ve percent of the FTI results, what we nd acceptable. In future work Navier-Stokes equations will be used instead of Euler equations to obtain results that are expected to be closer to the FTI results.

8. Conclusions and Recommendations

Relating the accuracy of the CFD and FTI results and doing this in a minimal timespan to gain con dence in the CFD results are the main issues of the paper. The pre-processing time is minimized by creating a three dimensional CAD model that can be easily adapted in combination with an automatic grid generation. Since the size of the domain was minimized keeping in mind that the model error in the CFD has to fall within the con dence interval of the FTI results, accuracy was guaranteed with a minimal computation time.
We show that the Euler calculations lead to an acceptable approximation of the FTI results (for corrected data we get within ve percent of the FTI results). However, there is plenty of space for improvement. The simpli ed engine model has an accuracy in Mach number that has to be increased. A next step is to perform CFD computations with Navier-Stokes equations to include viscous effects. These results will be compared with the present inviscid results that were corrected for two dimensional viscous effects to determine the most ef cient way to obtain data for each point of the steady symmetric ight envelope.

References

[1] M. Drela and H. Youngren. *XFOIL 6.94 User Guide*. MIT, Aero and Astro and Aerocraft, Inc., 10 December 2001.

[2] T. Fujita, Y. Ito, and K. Nakahashi. Computational uid dynamics evaluation of national aerospace laboratory experimental supersonic airplane in ascent. *Journal of Aircraft*, 39(2):359–364, March-April 2002.

[3] S.J. Hulshoff, J.A. Mulder, and H.W.M. Hoeijmakers. Estimation of aircraft dynamic parameters using euler computations and comparison with ight test data. In *Proceedings of the AIAA Atmospheric Flight Mechanics Conference*, number AIAA-96-3416, July 29-31, 1996.

[4] A. Jameson, W. Schmidt, and E. Turkel. Numerical solution of the euler equations by nite volume methods using runge-kutta time-stepping schemes. 1981.

[5] G.W. Milne, J.A. Mulder, M.W. Soijer, and S. Juliana. Maximum likelihood stability & control derivative identi cation of a cessna citation 2. In *Proceedings of the AIAA GNC, AFM and MST Conference*, number AIAA-01-4013, August 6-9, 2001.

[6] A. Patel. *Development of an Adaptive RANS Solver for Unstructured Meshes*. Phd thesis, Université Libre de Bruxelles, 2003.